P H Y S I C A L   R E V I E W   L E T T E R S

Complex Behavior of Fluid Lithium under Extreme Conditions

André Kietzmann and Ronald Redmer

Institut für Physik, Universität Rostock, D-18051 Rostock, Germany

Michael P. Desjarlais and Thomas R. Mattsson

Pulsed Power Sciences Center, Sandia National Laboratories, Albuquerque, New Mexico 87185-1186, USA

Lithium is a prototypical simple metal at standard conditions which is well described within the nearly free electron model. However, by changing the density towards expanded or compressed states, the electrical conductivity shows strong and partly unexpected variations. We have performed quantum molecular dynamics simulations for fluid lithium for a wide range of densities and temperatures in order to derive the equation of state, the electrical conductivity, and information about structural and electronic changes along the expansion or compression. Based on these results, we can give a consistent description of the electrical conductivity from the nonmetallic expanded fluid up to the degenerate electron liquid at high densities.

The electrical conductivity of matter varies over a vast range. Comparing the conductivity of pure metals with that of almost ideal insulators, a factor of about 10^{31} derives which is, besides the pressure, probably the widest variation that physical quantities can show [1]. Although the explanation of conduction phenomena in simple metals at normal conditions seems to be a rather elementary and straightforward problem, when the state of simple metals is continuously changed towards lower or higher densities, a strong variation of the electrical conductivity is observed which cannot be derived from simple models. The study of the transition between metals and insulators is the subject of intense, ongoing research because correlations, disorder, and thermal excitations have to be considered simultaneously in a consistent quantum many-particle approach [2].

For instance, a metal-to-nonmetal transition occurs if the metallic fluid is thermally expanded from the melting to the critical point due to an increased localization of electrons around ions [3]. Isentropic compression of fluid Li from ambient conditions up to high pressures of several megabar [4–6] has revealed that the electrical conductivity is by no means increasing but decreasing. The latter behavior is closely related to the predicted nonsimple, rich phase diagram of the solid alkali metals Li and Na at high pressures. Compression results in this case in a diminishing coordination number along a sequence of structural changes [7]. The insulating, dimerized Li ground state (*Cmca* or *oC*8 phase) as predicted by Neaton and Ashcroft [8] was later confirmed by Hanfland *et al.* [9] within density functional theory (DFT) using the generalized gradient approximation (GGA) for pressures above 165 GPa. For pressures between 48 and 165 GPa, they proposed the *cI*16 phase with an unusual multicenter bonding situation which could be verified by x-ray diffraction experiments at 44 GPa and about 200 K in the solid. A series of structural and electronic transitions has also been

derived from *ab initio* calculations for molten Na [10]. Especially, a strong reduction of the electrical conductivity driven by the opening of a pseudogap at 65 GPa has been found which reflects a change of bonding character from the *s* to the *p* type at high pressures.

To explain the strong changes of the electrical conductivity of simple fluid metals as a function of the density is, therefore, a challenge to quantum many-particle theory. We have performed extensive quantum molecular dynamics (QMD) simulations for fluid Li as a prototypical simple metal for a broad region of densities and temperatures, covering expanded and compressed states within the range $\varrho = (0.15\text{–}20)\varrho_0$, where $\varrho_0 = 0.54$ g/cm^3 is the Li density at standard conditions. We consider temperatures of several hundred up to 10^4 K, i.e., warm dense matter.

QMD simulations have been proven to successfully calculate the electronic, structural, thermodynamic, and optical properties of warm dense matter in a combined first-principles approach; see [11–16] for details. We have performed QMD simulations employing a finite temperature Fermi occupation of the electronic states using Mermin's approach (FT-DFT) [17], which is implemented in the plane wave density functional code VASP (Vienna *ab initio* simulation package) [18,19]. We consider 32–128 atoms with 3 electrons per atom in the simulation box and periodic boundary conditions. The electron wave functions are calculated using the all-electron projector augmented wave potentials [20,21] supplied with VASP [18,19], which yield more accurate conductivity results compared with other pseudopotentials. The exchange-correlation functional is calculated within GGA using the parametrization of Perdew, Burke, and Ernzerhof [22] as in Refs. [9,16].

The convergence of the thermodynamic quantities in QMD simulations is an important issue [23]. We have chosen a plane wave cutoff E_{cut} at 900 eV so that the pressure is converged within 2% accuracy. We have also

checked the convergence with respect to a systematic enlargement of the **k**-point set in the representation of the Brillouin zone. Higher-order **k** points modify the equation of state (EOS) data only within 2% relative to a one-point result, so we have restricted our EOS calculations to the Γ point. The simulations were performed for a canonical ensemble with temperature, volume of the simulation box, and particle number therein as given quantities. The ion temperature is controlled by a Nosé-Hoover thermostat. After several hundred time steps, the system is equilibrated, and the subsequent 400–1000 time steps are taken to calculate the EOS data as running averages. We have checked the existence of thermodynamic equilibrium carefully by analyzing the pair correlation functions and the stability of the pressure p, temperature T, and internal energy E.

The dynamic conductivity $\sigma(\omega)$ is derived from the Kubo-Greenwood formula [24,25]; for details, see Ref. [11]. The dc conductivity follows in the static limit $\omega \to 0$. We have used various point sets for the integration of the Brillouin zone to ensure that the conductivity was converged better than 20% over the entire density range. Each conductivity point represents an average over evaluations performed for 10–20 typical snapshots taken from the QMD runs for the EOS.

We compare our QMD simulation results with experimental data in Figs. 1 and 2. We find excellent agreement with quasi-isentropic shock-compression experiments of Bastea and Bastea [6], which cover a density range from $\varrho = (2–4)\varrho_0$ and temperatures from 2000 to 7000 K. In general, the agreement of the EOS data is better than 10%. The steep decrease of the conductivity up to 1 Mbar can be attributed to an increased scattering of the conduction electrons in compressed Li. An increasing effective mass in this region can be derived by balancing experimental data with an evaluation of the Ziman formula with m^* as free parameter [6].

We do not confirm the small drop in the conductivity at or above 1.8 Mbar which has been claimed to be a pre-

cursor of the pairing instability predicted for compressed solid Li [8] in the warm fluid regime. To the contrary, the plateau region extends smoothly up to almost 5 Mbar.

We next compare with a second series of multiple shock-compression experiments [4,5] in Fig. 2, which were performed in a similar density range $\varrho = (1–4.5)\varrho_0$ but at temperatures below 3000 K. Again, the conductivity isotherms derived from the QMD simulations cover the experimental data well for densities up to 1.7 g/cm^3. The decrease in conductivity with density coincides in this region with the experimental results of Ref. [6]. We do not reproduce the increase in conductivity above 1.8 g/cm^3 and the strong enhancement at about 2.3 g/cm^3 (i.e., four-fold compression). Instead of a sixfold increase, we find an almost temperature-independent conductivity in this high-density region, as can be seen from the merging isotherms. The 7000 K data point of Bastea and Bastea [6] supports our results. We conclude that novel experiments are necessary in order to confirm or challenge the high-pressure behavior of fluid Li predicted in this work.

We have performed further large-scale QMD simulations for fluid Li over a wide range of densities and temperatures in order to study the behavior of the electrical conductivity, the density of states (DOS), the ion-ion pair correlation function (PCF), and the charge density; see Figs. 3–6. We can identify three main regions.

(i) The *expanded fluid* (EF) is located at low densities $\varrho \lesssim \varrho_0/2$ and shows a strong increase of the conductivity with the density, almost independent of the temperature, and the DOS in Fig. 4 has a shape typical for nearly free electrons. Applying Mott's criterion for the minimum electrical conductivity of $\sigma_{min} = 2000/\Omega$ cm also for fluid alkali metals [1,3], the nonmetal-to-metal transition occurs at about 0.15 g/cm^3, i.e., just in the region where the critical point is probably located ($\varrho_c = 0.105$ g/cm^3 and $T_c = 3223$ K; see Ref. [26]). Electrons are increasingly delocalized due to the Mott effect, which plays a central role in chemical models and leads to pressure ionization; see Ref. [27] for details. The expanded fluid contains a
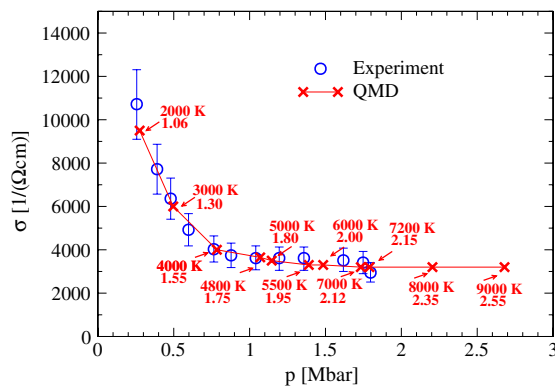

FIG. 1 (color online). Electrical conductivity of shock-compressed Li [6] compared with QMD simulations. The temperatures and densities (in g/cm^3) of the QMD calculations are indicated.
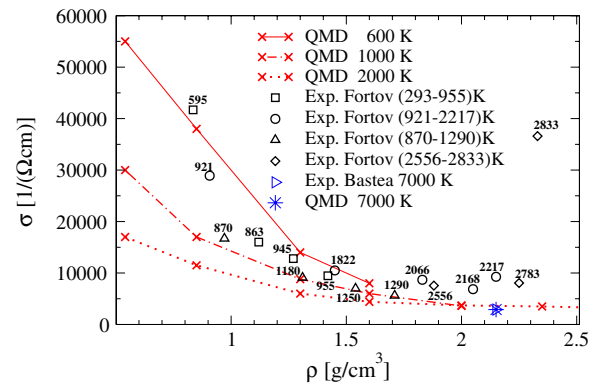

FIG. 2 (color online). Electrical conductivity of shock-compressed Li [4,5] compared with isotherms derived from QMD simulations. We have added the 7000 K data points from Fig. 1.
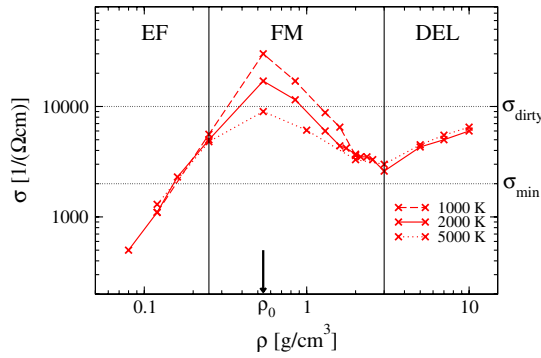
FIG. 3 (color online). General behavior of the electrical conductivity of fluid Li from low up to ultrahigh densities for various temperatures. EF: expanded fluid; FM: fluid metal; DEL: degenerate electron liquid.

FIG. 5 (color online). Ion-ion pair correlation function in fluid Li at 2000 K for a sequence of densities.

fraction of transient dimers and possibly other small neutral and charged clusters; see Figs. 5 and 6. Such a feature has been predicted within chemical models earlier [28] and demonstrated recently for Rb [29,30] by QMD simulations in this region.

(ii) The *fluid metal* (FM) can be identified in the range $\varrho_0/2 \leq \varrho \leq 5.5\varrho_0$ and shows a strong variation of the conductivity with the density. As typical for metals, the conductivity decreases with the temperature. After passing through a maximum at normal density ϱ_0, the conductivity decreases to values typical for a dirty metal below $\sigma_{\text{dirty}} = 10.000/\Omega$ cm [31]. Increasing density leads in this domain to a decreasing interatomic spacing and, thus, to stronger electron-ion scattering; see Figs. 5 and 6. Furthermore, the DOS in Fig. 4 is strongly reduced at the Fermi level as already found in Ref. [9]. Both effects diminish the conductivity in this region.

(iii) In the subsequent high-density region above 3 g/cm^3 (i.e., for more than sixfold compression), the conductivity increases systematically, again almost independent of temperature. This is typical for a *degenerate electron liquid* (DEL) where scattering becomes weaker

due to the strong screening effects and the Pauli exclusion principle, which prohibits scattering processes into occupied final states. The ions show a largely ordered structure already in this dense fluid regime reflecting a multicenter bonding situation; see Figs. 5 and 6. This was already anticipated by Neaton and Ashcroft [8] based on their results for the paired ground state of solid Li at high pressures. However, our results show that the DOS is relatively low in the DEL with a weak pseudogap at E_F (see Fig. 4), but the conductivity is still metal-like so that a completely paired, insulating ground state may occur only at much lower temperatures in the solid.

The drastic structural changes in fluid Li with increasing density are visualized by means of the PCF shown in Fig. 5. The next-neighbor distance decreases systematically with increasing density. Dimers Li$_2$ with a bond length of 2.7 Å (see [27]) can be identified in the expanded fluid up to densities above standard conditions by a peak in the PCF at the respective distance. The first peak and several smaller maxima for next neighbors subsequent fluid shells can be
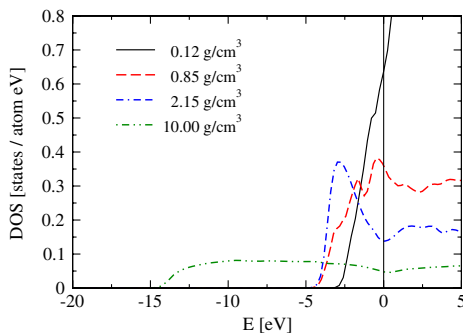

FIG. 4 (color online). Density of states in fluid Li at 2000 K for a sequence of densities with the Fermi energy located at zero energy. Increasing density leads to a strong reduction of the DOS at the Fermi level which is typical for a dirty metal. In the high-density limit, the DOS is almost constant which underlines the nonsimple metal behavior in this highly correlated region.
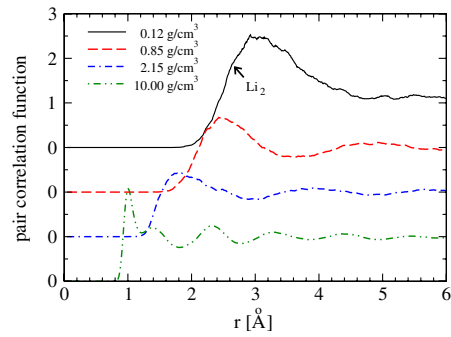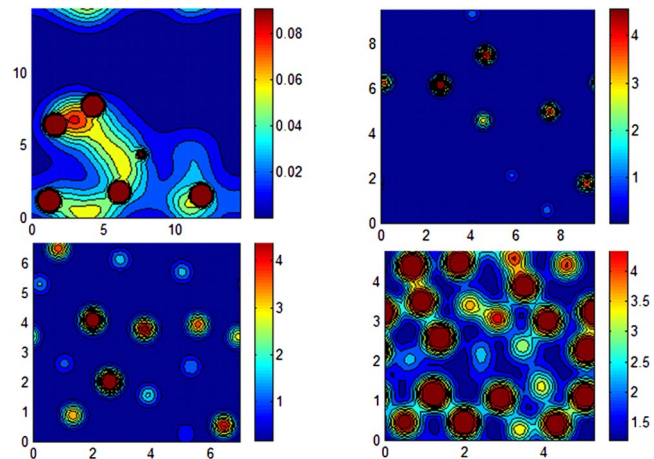

FIG. 6 (color online). Variation of the charge density in fluid Li at 2000 K in units of $e/\text{Å}^3$ for a sequence of densities (0.12 g/cm^3 upper left to 10.0 g/cm^3 lower right). The x and y axis are also given in units of Å. The charge density plots are taken from typical snapshots of the QMD run. We have selected representative planes through the simulation box parallel to the xy plane.

seen. This structure is thermally broadened with increasing temperature. While the fluid character is evident in, for example, long-range diffusive motion, the actual melting curve at high densities is of separate interest; see Ref. [32]. We calculate the melting temperature of Li at 2.7, 5.4, and 10.8 g/cm^3 to be below 1600 K. We can give the estimate (1250 ± 200) K; see [33].

We show the variation of the charge density in fluid Li with increasing density in Fig. 6. In the expanded fluid, small transient clusters can be seen as discussed above. The fluid metal is characterized by ions immersed in an almost homogeneous electron gas; the ions show no tendency for pairing or more complicated structures. Precursors of a lattice with a chainlike, dimeric structure are found in the high-density degenerate electron liquid. This can be related to the *s*- to *p*-type transition as found recently for Na [10] and solid Li [9].

In summary, we have determined the electrical conductivity of fluid lithium within QMD simulations over a broad range of densities and temperatures. The surprising complexity in the variation of the conductivity has been explained by analyzing the ion-ion PCF, the DOS, and structural changes. The agreement of our *ab initio* results with multiple shock-compression experiments is excellent for densities up to 1.7 [4,5] and 2.15 g/cm^3 [6]. We have identified three different density regions with specific physical properties: the expanded fluid for low densities, the fluid metal around normal densities, and the degenerate electron liquid at the highest densities. The electrical conductivity shows continuous transitions from nonmetallic to metallic behavior, a subsequent decrease to values typical for dirty metals, and an almost temperature-independent increase in the high-density limit. For the highest densities around 10 g/cm^3, we find precursors of a complex structure with chains of paired ions in the fluid phase at 2000 K. The calculation of the entire phase diagram including the location of the high-pressure melting line and the evaluation of complex high-density structures at finite temperatures is a topic of future work.

[1] P. P. Edwards, R. L. Johnston, C. N. R. Rao, D. P. Tunstall, and F. Hensel, Phil. Trans. R. Soc. A **356**, 5 (1998).

[2] D. E. Logan, Y. H. Szczech, and M. A. Tusch, in *Metal-Insulator Transitions Revisited*, edited P. P. Edwards and C. N. R. Rao (Taylor & Francis, London, 1995), pp. 343.

[3] F. Hensel and W. W. Warren, *Fluid Metals* (Princeton University Press, Princeton, 1999).

[4] V. E. Fortov *et al.*, JETP Lett. **70**, 628 (1999).

[5] V. E. Fortov *et al.*, J. Phys. Condens. Matter **14**, 10 809 (2002).

[6] M. Bastea and S. Bastea, Phys. Rev. B **65**, 193104 (2002).

[7] R. Rousseau, K. Uehara, D. D. Klug, and J. S. Tse, Chem. Phys. Chem. **6**, 1703 (2005).

[8] J. B. Neaton and N. W. Ashcroft, Nature (London) **400**, 141 (1999).

[9] M. Hanfland, K. Syassen, N. E. Christensen, and D. L. Novikov, Nature (London) **408**, 174 (2000).

[10] J. Y. Raty, E. Schwegler, and S. A. Bonev, Nature (London) **449**, 448 (2007).

[11] M. P. Desjarlais, J. D. Kress, and L. A. Collins, Phys. Rev. E **66**, 025401 (2002).

[12] M. P. Desjarlais, Phys. Rev. B **68**, 064204 (2003).

[13] Y. Laudernet, J. Clérouin, and S. Mazevet, Phys. Rev. B **70**, 165108 (2004).

[14] J. Clérouin, P. Renaudin, Y. Laudernet, P. Noiret, and M. P. Desjarlais, Phys. Rev. B **71**, 064203 (2005).

[15] T. R. Mattsson and M. P. Desjarlais, Phys. Rev. Lett. **97**, 017801 (2006).

[16] A. Kietzmann, B. Holst, R. Redmer, M. P. Desjarlais, and T. R. Mattsson, Phys. Rev. Lett. **98**, 190602 (2007).

[17] N. D. Mermin, Phys. Rev. **137**, A1441 (1965).

[18] G. Kresse and J. Hafner, Phys. Rev. B **47**, 558 (1993); **49**, 14 251 (1994).

[19] G. Kresse and J. Furthmüller, Phys. Rev. B **54**, 11 169 (1996).

[20] P. E. Blöchl, Phys. Rev. B **50**, 17 953 (1994).

[21] G. Kresse and D. Joubert, Phys. Rev. B **59**, 1758 (1999).

[22] J. P. Perdew, K. Burke, and M. Ernzerhof, Phys. Rev. Lett. **77**, 3865 (1996).

[23] A. E. Mattsson, P. A. Schultz, M. P. Desjarlais, T. R. Mattsson, and K. Leung, Model. Simul. Mater. Sci. Eng. **13**, R1 (2005).

[24] R. Kubo, J. Phys. Soc. Jpn. **12**, 570 (1957).

[25] D. A. Greenwood, Proc. Phys. Soc. London **71**, 585 (1958).

[26] V. E. Fortov, A. N. Dremin, and A. A. Leontev, Teplofiz. Vys. Temp. **13**, 984 (1975).

[27] R. Redmer, Phys. Rep. **282**, 35 (1997).

[28] R. Redmer and W. W. Warren, Jr., Phys. Rev. B **48**, 14 892 (1993).

[29] A. Kietzmann, B. Holst, R. Redmer, F. Hensel, M. P. Desjarlais, and T. R. Mattsson, J. Phys. Condens. Matter **18**, 5597 (2006).

[30] M. Ross, L. H. Yang, and W.-C. Pilgrim, Phys. Rev. B **74**, 212302 (2006).

[31] D. E. Logan, J. Chem. Phys. **94**, 628 (1991).

[32] I. Tamblyn, J.-Y. Raty, and S. A. Bonev, arXiv:0805.2781 [Phys. Rev. Lett. (to be published)].

[33] See EPAPS Document No. E-PRLTAO-101-042833 for the equation of state data and results for the melting temperature of fluid lithium at high pressures in addition to the results for the electrical conductivity, the density of states, the pair correlation function, and the charge density. For more information on EPAPS, see http://www.aip.org/pubservs/epaps.html.